# Reduced Smooth Muscle Contractile Capacity Facilitates Maladaptive Arterial Remodeling

## John F. Eberth<sup>1</sup>

Department of Cell Biology and Anatomy, Biomedical Engineering Program, University of South Carolina, Columbia, SC 29208 e-mail: john.eberth@uscmed.sc.edu

## Jay D. Humphrey

Fellow ASME
Department of Biomedical Engineering,
Yale University,
New Haven, CT 06520
e-mail: jay.humphrey@yale.edu

Albeit seldom considered explicitly, the vasoactive state of a central artery can contribute to luminal control and thereby affect the in vivo values of flow-induced wall shear stress and pressureinduced intramural stress, which in turn are strong determinants of wall growth and remodeling. Here, we test the hypothesis that diminished vasoactive capacity compromises effective mechanoadaptations of central arteries. Toward this end, we use consistent methods to re-interpret published data on common carotid artery remodeling in a nonpharmacologic mouse model of induced hypertension and a model of connective tissue disorder that results in Marfan syndrome. The mice have identical genetic backgrounds and, in both cases, the data are consistent with the hypothesis considered. In particular, carotid arteries with strong (normal) vasoactive capacity tend to maintain wall thickness and in vivo axial stretch closer to homeostatic, thus resulting in passive circumferential wall stress and energy storage close to normal. We conclude that effective vasoactivity helps to control the biomechanical state in which the cells and matrix turnover, thus helping to delineate mechano-adaptive from maladaptive remodeling. Future analyses of experimental data and computational models of growth and remodeling should account for this strong coupling between smooth muscle contractile capacity and central arterial remodeling. [DOI: 10.1115/1.4052888]

 $\label{lem:keywords: hypertension, Marfan syndrome, extracellular matrix remodeling, stiffness, phenotype$ 

#### 1 Introduction

Arteries exhibit a remarkable ability to adapt to changing hemodynamic loads, acutely via vasoactive changes that regulate luminal caliber and chronically via a turnover of cells and matrix within vaso-altered states that often modifies the geometry, composition, properties, and function [1,2]. Complementary roles of vasoactivity and arterial remodeling are well-known in the smallest arteries, that is, arterioles [3,4], but there has been much less attention to similar relationships in central arteries. Central arterial remodeling is fundamental, of course, to cardiovascular health and diverse diseases [5], and thus merits continued investigation.

We recently reported a novel observation in the descending thoracic aorta of wild-type mice rendered hypertensive via two-tofour weeks of infusion of angiotensin II, namely, a remarkable spectrum of arterial remodeling ranging from near adaptive to

grossly maladaptive [6]. The maladaptive aortas were characterized histopathologically by a dramatic over-thickening of the wall, primarily via marked accumulations of medial and especially adventitial collagen. Immuno-staining revealed modest decreases in the maladapted aortas in smooth muscle  $\alpha$ -actin and smooth muscle myosin heavy chain, two key markers of a contractile phenotype [7]. Importantly, however, vessel-level vasoconstriction was significantly impaired in the maladapted aortas and we uncovered a strong correlation between the degree of maladaptation, reflected by aberrant wall thickening and loss of mechanical functionality, and diminishing vasoconstrictive capacity. This observation may be thought to simply reflect a modulation from a contractile-to-synthetic phenotype consistent with the increase in matrix, but it also emphasizes the importance of smooth muscle contractile capacity in determining the biomechanical state in which the cells and matrix turnover. In particular, given the longstanding observation that the degree of vascular growth and remodeling depends in large part on deviations in flow-induced wall shear stress  $\tau_w$  and pressure-induced intramural stress  $\sigma_{\theta}$  from normal homeostatic values [8], it is critical to note that smooth muscle cell contractile capacity contributes directly to both of these stresses, mean values of which can be calculated via

$$au_w = rac{4\mu Q}{\pi a(P,C)^3}, \quad \sigma_\theta = rac{Pa(P,C)}{h(P,C)}$$

where a is the deformed luminal radius and h the deformed wall thickness, with  $\mu$  the dynamic viscosity, Q the volumetric flowrate, P the pressure, and C the contractility, thus emphasizing both the (passive) pressure and the (active) contractile control of geometry and thus stress.

Although chronic infusion of angiotensin II is commonly used to induce hypertension in mice, exogenous angiotensin not only increases blood pressure, it is also highly pro-inflammatory and inflammation can play a key role in the associated aortic remodeling [9,10]. In this technical brief, we test the hypothesis that the aforementioned strong correlation between maladaptive aortic wall remodeling and diminished smooth muscle contractile capacity holds in another well-accepted mouse model of hypertension that is driven by altered hemodynamics, not exogenously stimulated inflammation, and it similarly holds for a different central artery. Noting that diminished smooth muscle cell contractility also manifests in central arteries of mouse models of compromised elastic fiber integrity [11,12], we also contrasted carotid properties and smooth muscle contractility in a mouse model of Marfan syndrome.

#### 2 Methods

The data upon which we base the present analyses were reported previously for adult male mice [13–15]. Briefly, in the first of these studies, a ligature was placed around the aorta between the brachiocephalic and left common carotid arteries, thus locally constricting the aortic arch and increasing pulse pressure in the right common carotid artery relative to both the contralateral left common carotid artery and control carotids. The carotid arteries were excised either before (n = 18) or at multiple times after a rtic constriction (n = 4 at 7 days, n = 5 at 10 days, n = 4 at 14 days, and n = 7 at 35–56 days), then biomechanically phenotyped via a series of active protocols to assess smooth muscle (in response to  $10^{-5}$  M phenylephrine) and endothelial ( $10^{-5}$ M carbamylcholine chloride) function as well as multiple passive  $(10^{-5} \text{ M sodium nitroprusside and EGTA 2} \times 10^{-3} \text{ M})$  pressurediameter and axial force-length protocols to quantify the passive biaxial mechanical properties. In the second of these studies, common carotid arteries were excised from a mouse model of Marfan syndrome (MFS), thus allowing assessments of the effects of heterozygous  $(Fbn1^{mgR/+})$  and homozygous  $(Fbn1^{mgR/mgR})$  mutations that reduce the amount of normal fibrillin-1 [16]. Noting that fibrillin-1 is an elastin-associated glycoprotein that contributes

<sup>&</sup>lt;sup>1</sup>Corresponding author.

Manuscript received May 17, 2021; final manuscript received October 14, 2021; published online December 15, 2021. Assoc. Editor: Katherine Yanhang Zhang.

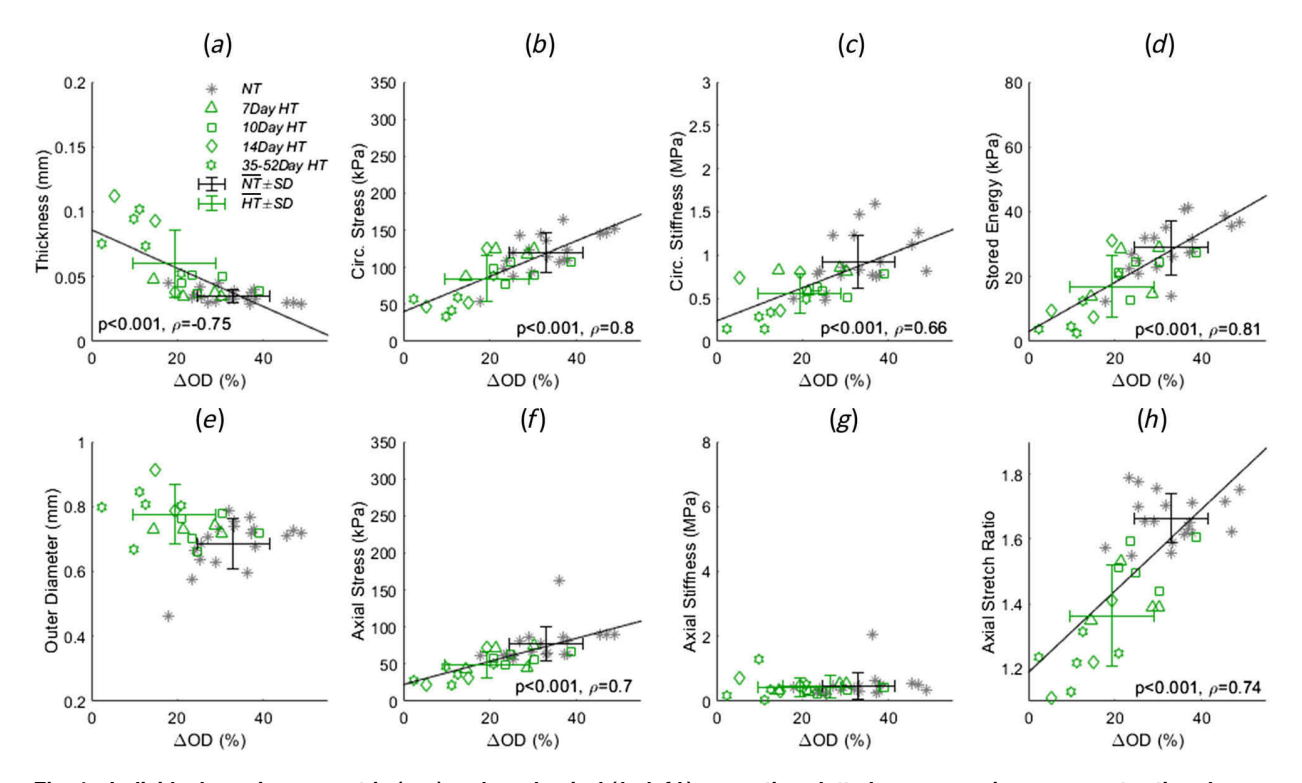


Fig. 1 Individual passive geometric (a, e) and mechanical (b-d, f-h) properties plotted versus maximum percent active change in outer diameter  $(\Delta OD)$  for common carotid arteries from mice 7 (n=4), 10 (n=5), 14 (n=4), or 35–56 (n=7) days following transverse aortic constriction surgery resulting in local systolic hypertension (HT) or pooled normotensive (NT; n=18) contralateral vessels. The maximally active contracted and passive diameters were recorded after adding, respectively, phenylephrine (PE) and later sodium nitroprusside (SNP) plus EGTA to the specimen bath while the vessels were pressurized at 80 mmHg and held at their individual in vivo axial stretch ratio. Mean values  $\pm$  SD for the NT and HT groups are shown as black and green bars, respectively. The best-fit linear regression models for the pooled NT and HT data are shown using Pearson's correlation for statistically significant-strong (p < 0.05 and |p| > 0.5 - solid lines) correlations. Statistically significant-moderate (p < 0.1 and |p| > 0.35) correlations were also tested and plots without regression lines failed to reach significance at either level.

both to elastic fiber stability and to mechanosensing, we studied carotids from 17 Fbn1 mice  $(n=6\ Fbn1^{+/+},\ n=4\ Fbn1^{mgR/+},\ and\ n=7\ Fbn1^{mgR/mgR})$ . Only vessels that demonstrated uniform endothelial and smooth muscle function in response to vasoreactants and completed biaxial mechanical testing are included herein. Thus sample sizes and experimental results differ slightly from prior reports [13–15].

Consistent with the aforementioned study on angiotensin IIinduced hypertensive remodeling of the thoracic aorta, we used the same four-fiber family constitutive model [6,15,17] to quantify passive metrics that reflect the biomechanical phenotype. These include biaxial wall stress, material stiffness, and energy storage under consistent conditions for a common distending pressure of 100 mmHg and the group-specific energetically preferred value of the in vivo axial stretch ratio. The associated best-fit values of the material parameters were determined via nonlinear regression to minimize the sum-of-the-squares differences between experimentally measured and theoretically calculated pressure and axial force. The percent change in outer diameter or axial force were calculated as  $100 \times |passive\ value - contracted\ value|/|passive\ value|$  with the contracted and passive values represented by the response to phenylephrine and sodium nitroprusside plus EGTA, respectively. Passive metrics were then plotted versus the specimen-specific maximum percent active change in diameter or force under isobaric and axially isometric conditions. Possible correlations were assessed using the Pearson correlation coefficient,  $\rho$ , with statistical significance indicated as strong (p < 0.05 and  $|\rho| > 0.5$ —solid lines) or moderate (p < 0.1 and  $|\rho| > 0.35$ ).

# 3 Results

Figure 1 shows measured or computed specimen-specific values of passive wall thickness, outer diameter, circumferential and

axial wall stress, circumferential and axial material stiffness, stored energy, and the in vivo axial stretch ratio as a function of the maximum vasoconstrictive reduction in outer diameter at 0 (i.e., normotensive controls), 7, 10, 14, or 35+ days after transverse aortic constriction. Amongst the eight metrics shown, note, in particular, the following mean normotensive values at  $100 \text{ mmHg: } 35.0 \pm 0.53 \,\mu\text{m} \text{ (wall thickness), } 1.68 \pm 0.07 \text{ (in vivo)}$ axial stretch ratio),  $0.12 \pm 0.03$  MPa (circumferential stress),  $28.9 \pm 8.21$  kPa (stored energy), and  $32.9 \pm 8.43\%$  (percent vasoactive change in outer diameter). As it can be seen, when considering the longitudinal hypertensive data together with their control data, there were multiple strong correlations ( $|\rho| > 0.05$ , p < 0.05) between passive metrics and the degree of vasoconstriction, with values of wall thickness higher ( $\rho = -0.75$ ; Fig.1(a)) and in vivo axial stretch ratio lower ( $\rho = 0.74$ ; Fig. 1(h)), circumferential ( $\rho = 0.80$ ; Fig. 1(b)) and axial ( $\rho = 0.70$ ; Fig. 1(f)) wall stress lower, and energy storage lower ( $\rho = 0.81$ ; Fig. 1(d)) than normal in cases of low vasoconstriction. The lower than homeostatic values of passive circumferential wall stress in cases of low smooth muscle contractility suggested a failed mechanoadaptation, resulting from an over-thickening of the wall given the pressure elevation and a decrease in the in vivo axial stretch ratio. Importantly, this failed mechano-adaptation in cases of low smooth muscle contractility is also associated with a dramatic loss of energy storage ability, noting that energy storage represents a key functionality of central arteries. Interestingly, correlations were absent for axial stiffness (Fig. 1(g)) but present for circumferential stiffness (Fig. 1(c)), which is generally a highly mechano-regulated quantity in central arteries [18,19], even in hypertension [10].

Figure 2 shows similar data for carotid arteries from control, heterozygous, and homozygous mice with fibrillin-1 deficiency.

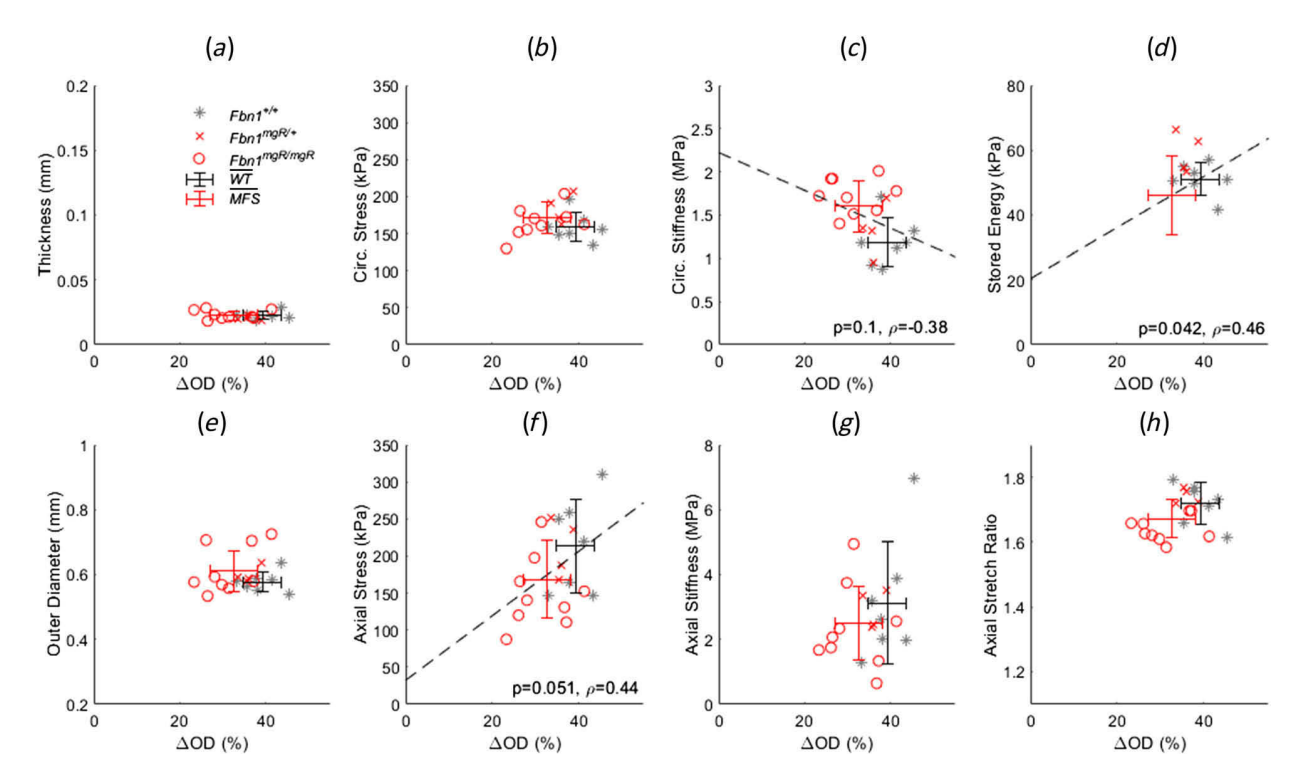


Fig. 2 Individual passive geometric (a, e) and mechanical (b-d, f-h) properties plotted versus maximum percent active change in outer diameter ( $\Delta OD$ ) of carotid arteries from  $Fbn1^{mgR/+}$  (n = 4) and  $Fbn1^{mgR/mgR}$  (n = 9) Marfan Syndrome (MFS) mice and their wild-type (WT)  $Fbn1^{+/+}$  (n = 7) controls. The mean values  $\pm$  SD for WT and MFS mice are shown as black and red bars, respectively. The best-fit linear regression models are shown using Pearson's correlation for the pooled WT and MFS data when statistically significant moderate correlations (p<0.1 and  $|\rho|$ >0.35 - dashed lines) were found. Statistically significant-strong (p<0.05 and  $|\rho|$ >0.5 - solid lines) correlations were also tested and plots without regression lines failed to reach significance at either level.

Trends for energy storage ( $\rho$  = 0.46; Fig. 2(d)) and axial wall stress ( $\rho$  = 0.44; Fig. 2(f)) were similar to those in Fig. 1, but the correlations were not as strong as in the case of aortic constriction. For circumferential stiffness ( $\rho$  = -0.38; Fig. 2(c)), the statistically significant but moderate trends were reversed from those seen in aortic constriction. It is well known that circumferential stiffness tends not to be mechano-regulated well in cases of thoracic aortopathy [10], including MFS. On average, the Marfan carotid arteries had a greater vasoactive capability (32.7% in terms of reduction in diameter) than did the hypertensive carotids (19.3%), though less than their wild-type (39%) controls.

In addition to inducing a change in outer diameter, the exchange of vasoreactants resulted in a net change in the axial force required to maintain the vessel at a fixed length during pressurization; this is thought to be due to the helical arrangement of smooth muscle cells in the media [7]. When data from the hypertensive carotids and their normotensive controls were plotted against measured or computed specimen-specific values of passive geometry or mechanics (Fig. 3), a strong relationship emerged between the maximum percent change in axial force and circumferential stress ( $\rho = 0.60$ ; Fig. 3(b)) and circumferential stiffness ( $\rho = 0.58$ ; Fig. 3(c)), with weak correlations with wall thickness ( $\rho = -0.45$ ; Fig 3(a)) and axial stretch ( $\rho = 0.46$ ; Fig. 3(h); no such correlations were found for these passive metrics for the Marfan group (data not shown). Likewise, no significant differences were found for the mean values of the change in axial force between the hypertensive and Marfan groups.

Histological analysis of HT carotids revealed a progressive wall thickening with time largely due to cell proliferation, glycosaminoglycan accumulation, and collagen accumulation, especially in the adventitia (quantified in [13,14]). Moreover, an inflammatory response progressed with remodeling time based on measurements of monocyte chemoattractant protein-1 (MCP-1), also shown

previously. Figure 4 displays representative histological features of HT and NT vessels stained with Hematoxylin and Eosin (H&E) or Picro-Sirius Red (PSR); both stains suggested an outward, hypertrophic remodeling response based on increases in the inner diameter and wall thickness [14]. In contrast, carotids from Marfan mice and wild-type controls were histologically similar when compared in brightfield images using H&E or the elastic fiber stain, Verhoeff-Van Gieson (VVG; Fig. 5). This is not surprising given the mild mechanical phenotype observed in the carotid arteries of these mice [15].

#### 4 Discussion

Prior findings in the thoracic aorta of hypertensive mice revealed a strong correlation between overall arterial remodeling and smooth muscle contractile capacity [6]. This finding was interpreted primarily as reflecting graded reductions in the pressure-induced circumferential wall stress via differential degrees of smooth muscle cell contraction, thus implicating a stress-driven remodeling of the wall that ranged from adaptive (with strong contractility) to maladaptive (with poor or absent contractility), consistent with both a prior theoretical biomechanical prediction [20] and a recent model of immuno-mechanical mediation of remodeling [21]. The present data for both a different central artery (common carotid) and different mouse models (a model of induced hypertension and a model of a connective tissue disorder) are consistent with the prior finding, thus supporting the associated hypothesis.

Prior studies by Stergiopulos and colleagues focused on the common carotid artery in a rat model of hypertension induced by an aortic constriction between the renal arteries [22,23]. They measured active and passive biomechanical properties over short (7 days) and longer (56 days) periods and reported that

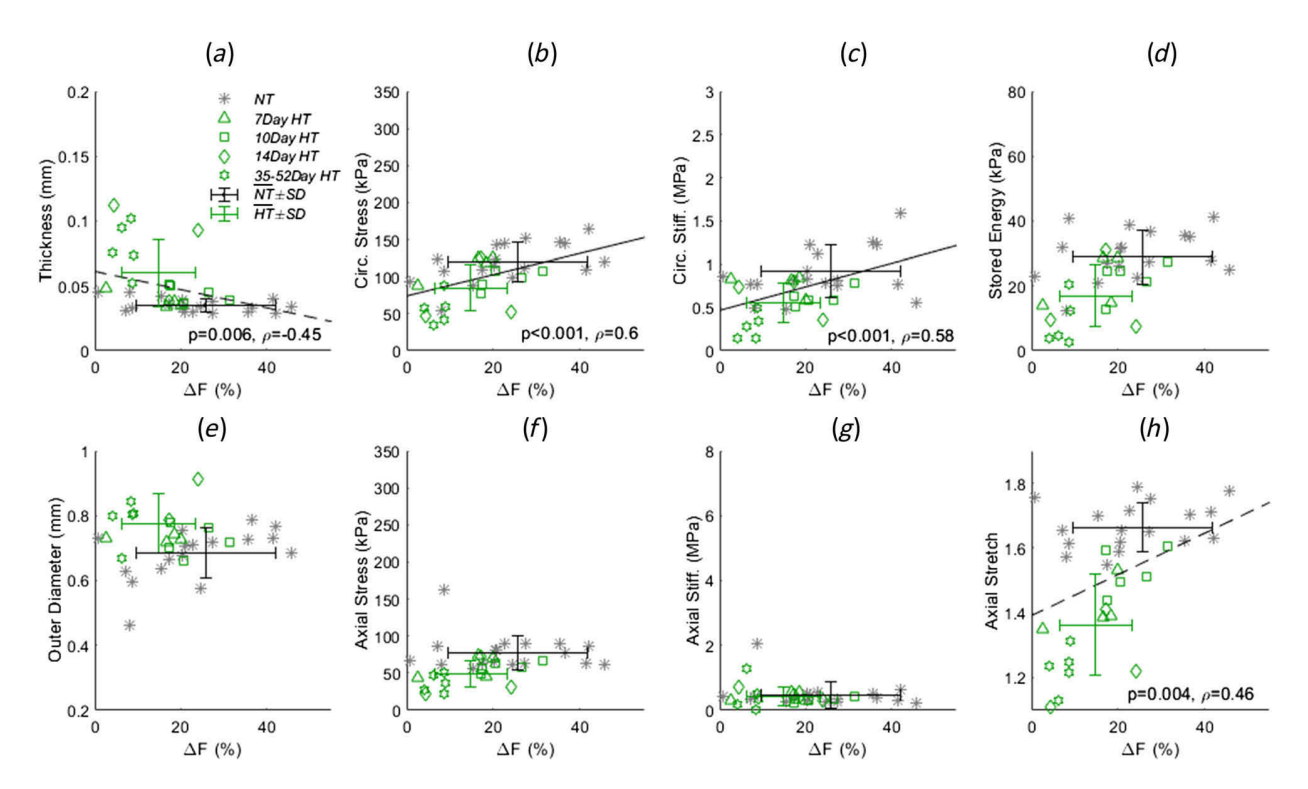


Fig. 3 Individual passive geometric (a, e) and mechanical (b-d, f-h) properties plotted versus maximum percent change in active axial force ( $\Delta F$ ) of carotid arteries taken from mice 7 (n = 4), 10 (n = 5), 14 (n = 4), and 35–56 (n = 7) days following transverse aortic coarctation surgery resulting in local systolic hypertension (HT) or their pooled normotensive (NT; n = 18) contralateral vessels. The maximally contracted and passive axial forces were recorded after adding phenylephrine (PE) and later sodium nitroprusside (SNP) with EGTA to the media respectively at 80 mmHg and the in vivo axial stretch ratio. The mean values±SD for the NT and HT groups are shown as black and green bars, respectively. The best-fit linear regression models for the pooled NT and HT data together are shown using Pearson's correlation when statistically significant-strong (p<0.05 and |p|>0.5 - solid lines) or moderate correlations (p<0.1 and |p|>0.35) were found. Plots without regression lines failed to reach significance at either level.

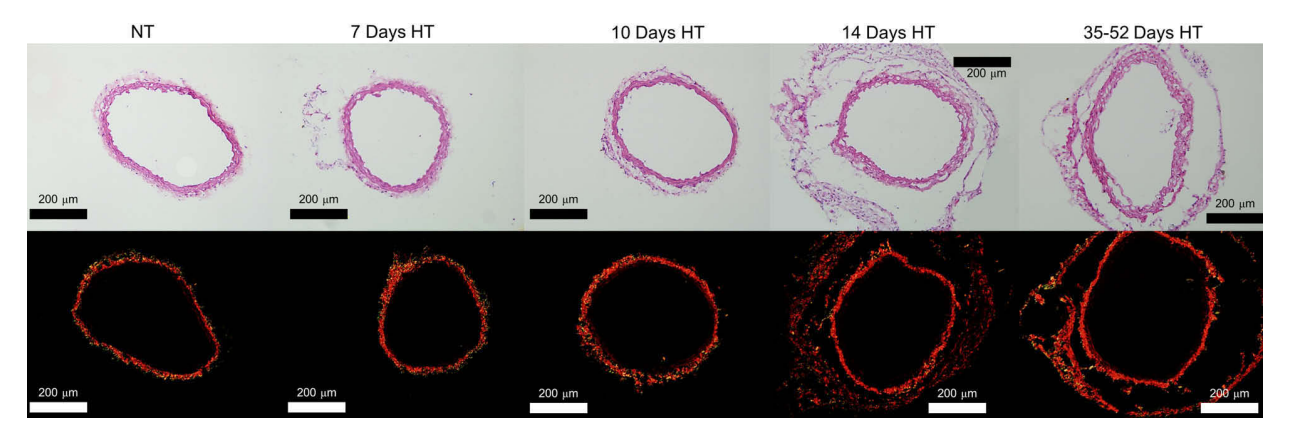


Fig. 4 (Left-to-right) Representative histological images of common carotid arteries from normotensive (NT) mice or 7, 10, 14, or 35–56 days following transverse aortic constriction surgery resulting in local systolic hypertension (HT). (Top) Hematoxylin and Eosin (H&E) stained brightfield images and (bottom) Picro-Sirius Red (PSR) stained darkfield images using cross-polarized light to illustrate collagen through birefringence. Scale bars are 200  $\mu$ m. The medial-adventitial separations after 14 days of HT reflect an important sectioning artifact, revealing an underlying structural vulnerability at this interface.

contractile capacity was increased during the short term but restored toward normal over the long-term, with near mechano-adaptation based on restoration of wall stress toward normal. Hence, their findings of a robust vasoactive capability associating with mechano-adaptation are consistent with our findings, though two apparent differences are noted. First, although they induced hypertension in 8–9-week-old male rats, wall thickness and inner radius increased disproportionally during the 8-week study period

in the control animals, thus resulting in a progressive increase in circumferential wall stress given the near-constant mean arterial pressure, implying that wall stress was not yet homeostatic at the beginning of the experiments. We recently showed that the aorta reaches biomechanical maturity by 8 weeks in the mouse [24]. Second, they did not report any gross over-thickening, and thus no maladaptation, which may have resulted from the different species or methods of inducing hypertension.

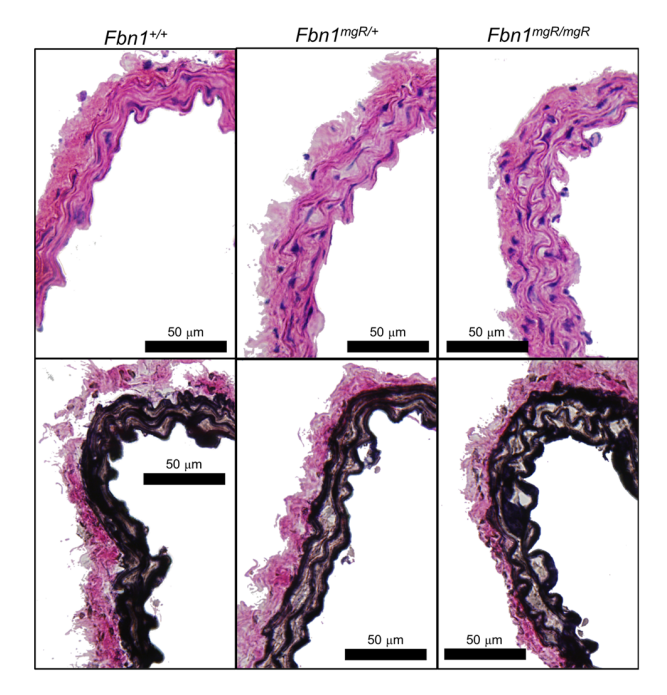


Fig. 5 (Left-to-right) Representative histological images of carotid arteries from  $Fbn1^{+/+}$ ,  $Fbn1^{mgR/+}$ , and  $Fbn1^{mgR/mgR}$  mice, respectively. (Top) Hematoxylin and Eosin-H&E and (bottom) Verhoeff Van Gieson-VVG stained cross section. Scale bars are 50  $\mu$ m.

Microscopic, morphological, and mechanical data from our prior study on the time course of carotid artery remodeling following transverse aortic constriction showed that HT vessels undergo outward and hypertrophic remodeling through an accumulation of extracellular matrix (collagen and ground substance) and cellular mass [14]. Although it is not possible to infer causality from such data given the absence of immunostaining for contractile proteins and lack of identification of signaling pathways, the current findings, in combination with our prior histo-mechanical data, are consistent with a failed stress-mediated remodeling response. Indeed, Kuang et al. [25] reported central artery (ascending aorta) remodeling following transverse constriction of the aortic arch, also noting a gross over-thickening (maladaptation) with related inflammatory involvement evidenced by increased MCP-1 and interleukin-6 (IL-6). The dataset from which we took the hypertensive data did not measure the presence of inflammatory cells or inflammatory cytokines such as IL-6, but did report a progressive increase in MCP-1 with an associated marked adventitial accumulation of collagen [14]. It is likely, therefore, that those vessels that maladapted had inflammatory cell involvement, not unlike that in angiotensin II infusion models (cf. [9,10]). Importantly, there is increasing evidence that excessive wall stresses may serve as a stimulus for inflammation, thus suggesting that the mechanoadaptive responses seen in vessels with greater smooth muscle cell contractile capacity may have resulted from a contractionassociated reduction in wall stress below a threshold value that is needed to stimulate inflammation [21]. This provocative hypothesis merits further investigation.

Whereas our original observation was for aortic remodeling in the context of hypertension [6], we sought herein to test our hypothesis in another central artery, the common carotid, using both a different model of induced hypertension and a connective tissue disorder in which vasocontractility is compromised [13–15]. The latter (MFS) included a more modest reduction in vasoconstrictive capacity and no appreciable difference in blood pressure. Rather, any altered mechano-mediation of wall geometry and properties was expected due to compromised mechanosensing, which is emphasized in the ascending aorta and much

less so in the common carotid artery [11,15]. Trends in a few of the key metrics were nonetheless consistent with the current hypothesis, although not as strongly correlated, likely due to the lack of a strong mechano-stimulus. Considering that the mean values of circumferential stress were similar between MFS and wild-types, the mechano-stimulus was likely sensed well by these cells.

In summary, although causality is difficult to establish in vascular mechanics and mechanobiology, the present findings support complementary findings in the literature that suggest that diminished smooth muscle cell contractile capacity can contribute to maladaptive central artery remodeling due to a failure to reduce wall stress to levels that allow effective mechanoadaptive remodeling. Given that vasodilators can be used to treat hypertension and reduce the hemodynamic load in patients afflicted with Marfan syndrome, our findings support the speculative hypothesis that it will be beneficial to preserve contractility in large arteries while reducing it in arterioles, the former to protect against maladaptive remodeling and the latter to reduce increases in total peripheral resistance that drive hypertension via an insidious feedback loop [5].

#### **Funding Data**

US National Institutes of Health (P01 HL134605, R03 EB031123, R01 HL145064; Funder ID: 10.13039/100000002).

National Science Foundation (CMMI 1760906; Funder ID: 10.13039/100000001).

#### References

- Dajnowiec, D., and Langille, B. L., 2007, "Arterial Adaptations to Chronic Changes in Haemodynamic Function: Coupling Vasomotor Tone to Structural Remodelling," Clin. Sci., 113(1), pp. 15–23.
- [2] Valentín, A., Cardamone, L., Baek, S., and Humphrey, J. D., 2009, "Complementary Vasoactivity and Matrix Remodelling in Arterial Adaptations to Altered Flow and Pressure," J. R. Soc. Interface, 6(32), pp. 293–306.
- [3] Bakker, E. N. T. P., van der Meulen, E. T., van den Berg, B. M., Everts, V., Spaan, J. A. E., and VanBavel, E., 2002, "Inward Remodeling Follows Chronic Vasoconstriction in Isolated Resistance Arteries," J. Vasc. Res., 39(1), pp. 12–20.
- [4] Martinez-Lemus, L. A., Hill, M. A., Bolz, S. S., Pohl, U., and Meininger, G. A., 2004, "Acute Mechanoadaptation of Vascular Smooth Muscle Cells in Response to Continuous Arteriolar Vasoconstriction: Implications for Functional Remodeling," Faseb J., 18(6), pp. 708–710.
- [5] Laurent, S., and Boutouyrie, P., 2015, "The Structural Factor of Hypertension: Large and Small Artery Alterations," Circ. Res., 116(6), pp. 1007–1021.
- [6] Korneva, A., and Humphrey, J. D., 2019, "Maladaptive Aortic Remodeling in Hypertension Associates With Dysfunctional Smooth Muscle Contractility," Am. J. Physiol. Circ. Physiol., 316(2), pp. H265–H278.
- [7] Zhou, B., Prim, D. A., Romito, E. J., McNamara, L. P., Spinale, F. G., Shazly, T., and Eberth, J. F., 2018, "Contractile Smooth Muscle and Active Stress Generation in Porcine Common Carotids," ASME J. Biomech. Eng., 140(1), p. 014501.
- [8] Humphrey, J. D., 2008, "Mechanisms of Arterial Remodeling in Hypertension Coupled Roles of Wall Shear and Intramural Stress," Hypertension, 52(2), pp. 195–200.
- [9] Wu, J., Thabet, S. R., Kirabo, A., Trott, D. W., Saleh, M. A., Xiao, L., Madhur, M. S., Chen, W., and Harrison, D. G., 2014, "Inflammation and Mechanical Stretch Promote Aortic Stiffening in Hypertension Through Activation of P38 Mitogen-Activated Protein Kinase," Circ. Res., 114(4), pp. 616–625.
- [10] Bersi, M. R., Khosravi, R., Wujciak, A. J., Harrison, D. G., and Humphrey, J. D., 2017, "Differential Cell-Matrix Mechanoadaptations and Inflammation Drive Regional Propensities to Aortic Fibrosis, Aneurysm or Dissection in Hypertension," J. R. Soc. Interface, 14(136), p. 20170327.
- [11] Chung, A. W. Y., Au Yeung, K., Sandor, G. G. S., Judge, D. P., Dietz, H. C., and Van Breemen, C., 2007, "Loss of Elastic Fiber Integrity and Reduction of Vascular Smooth Muscle Contraction Resulting From the Upregulated Activities of Matrix Metalloproteinase-2 and -9 in the Thoracic Aortic Aneurysm in Marfan Syndrome," Circ. Res., 101(5), pp. 512–522.
- [12] Murtada, S.-I., Ferruzzi, J., Yanagisawa, H., and Humphrey, J. D., 2016, "Reduced Biaxial Contractility in the Descending Thoracic Aorta of Fibulin-5 Deficient Mice," ASME J. Biomech. Eng., 138(5), p. 051008.
- [13] Eberth, J. F., Gresham, V. C., Reddy, A. K., Popovic, N., Wilson, E., and Humphrey, J. D., 2009, "Importance of Pulsatility in Hypertensive Carotid Artery Growth and Remodeling," J Hypertens, 27(10), pp. 2010–2021.
- [14] Eberth, J. F., Popovic, N., Gresham, V. C., Wilson, E., and Humphrey, J. D., 2010, "Time Course of Carotid Artery Growth and Remodeling in Response to

- Altered Pulsatility," Am. J. Physiol. Heart Circ. Physiol., 299(6), pp. H1875–H1883.
- [15] Eberth, J. F., Taucer, A. I., Wilson, E., and Humphrey, J. D., 2009, "Mechanics of Carotid Arteries in a Mouse Model of Marfan Syndrome," Ann. Biomed. Eng., 37(6), pp. 1093–1104.
- [16] Marque, V., Kieffer, P., Gayraud, B., Lartaud-Idjouadiene, I., Ramirez, F., and Atkinson, J., 2001, "Aortic Wall Mechanics and Composition in a Transgenic Mouse Model of Marfan Syndrome," Arterioscler., Thromb., Vasc. Biol., 21(7), pp. 1184–1189.
- [17] Prim, D. A., Lane, B. A., Ferruzzi, J., Shazly, T., and Eberth, J. F., 2021, "Evaluation of the Stress-Growth Hypothesis in Saphenous Vein Perfusion Culture," Ann. Biomed. Eng., 49(1), pp. 487–501.
- [18] Shadwick, R. E., 1999, "Mechanical Design in Arteries," J. Exp. Biol., 202(23), pp. 3305–3313.
- [19] Bersi, M. R., Ferruzzi, J., Eberth, J. F., Gleason, R. L., Jr., and Humphrey, J. D., 2014, "Consistent Biomechanical Phenotyping of Common Carotid Arteries From Seven Genetic, Pharmacological, and Surgical Mouse Models," Ann. Biomed. Eng, 42(6), pp. 1207–1223.
- [20] Wilson, J. S., Baek, S., and Humphrey, J. D., 2013, "Parametric Study of Effects of Collagen Turnover on the Natural History of Abdominal

- Aortic Aneurysms," Proc. R. Soc. A Math. Phys. Eng. Sci., **469**(2150), p. 20120556.
- [21] Latorre, M., Spronck, B., and Humphrey, J. D., 2021, "Complementary Roles of Mechanotransduction and Inflammation in Vascular Homeostasis," Proc. R. Soc. A, 477(2245), p. 20200622.
- [22] Fridez, P., Makino, A., Kakoi, D., Miyazaki, H., Meister, J. J., Hayashi, K., and Stergiopulos, N., 2002, "Adaptation of Conduit Artery Vascular Smooth Muscle Tone to Induced Hypertension," Ann. Biomed. Eng., 30(7), pp. 905–916.
- [23] Fridez, P., Makino, A., Miyazaki, H., Meister, J.-J., Hayashi, K., and Stergiopulos, N., 2001, "Short-Term Biomechanical Adaptation of the Rat Carotid to Acute Hypertension: Contribution of Smooth Muscle," Ann. Biomed. Eng., 29(1), pp. 26–34.
- [24] Murtada, S.-I., Kawamura, Y., Li, G., Schwartz, M. A., Tellides, G., and Humphrey, J. D., 2021, "Developmental Origins of Mechanical Homeostasis in the Aorta," Dev. Dyn., 250(5), pp. 629–639.
- [25] Kuang, S.-Q., Geng, L., Prakash, S. K., Cao, J.-M., Guo, S., Villamizar, C., Kwartler, C. S., Peters, A. M., Brasier, A. R., and Milewicz, D. M., 2013, "Aortic Remodeling After Transverse Aortic Constriction in Mice is Attenuated With AT1 Receptor Blockade," Arterioscler. Thromb. Vasc. Biol., 33(9), pp. 2172–2179.